Hindawi
Advances in Civil Engineering
Volume 2022, Article ID 5845340, 11 pages
https://doi.org/10.1155/2022/5845340

Research Article

The Influence of Water-Level Fluctuation on the Instability and Seepage Failure of Dump-Fill Cofferdam

Yunqing Hu,[1] Jianyu Huang,[2] Zhipeng Tao,[3] Junhua Zhu,[4] Qing Lv,[5] Jianwei Qiao,[6] and Weibin Cai[7]

[1]*Jiangxi V&T College of Communications, Nanchang 330062, China*
[2]*Nanchang Longxing Port Group Co., Ltd., Nanchang 330062, China*
[3]*Jiangxi Transportation Institute Co., Ltd., Nanchang 330062, China*
[4]*School of Civil Engineering and Architecture, East China Jiaotong University, Nanchang 330013, China*
[5]*Research & Development Centre for Underground Technology of Jiangxi Province, Nanchang 330013, China*
[6]*China Jikan Research Institute of Engineering Investigations and Design Co., Ltd., Xi'an 710043, China*
[7]*Sichuan Highway Planning,Survey,Design and Research Institute Ltd., Chengdu 610047, China*

Correspondence should be addressed to Junhua Zhu; 3062@ecjtu.edu.cn

Received 1 December 2021; Accepted 18 March 2022; Published 12 April 2022

Academic Editor: Lingkun Chen

Due to the double disturbance effect of dredging and filling, there will be a problem with weir slope stability after the formation of a fill type saturated clay weir. In order to study the influence of water-level fluctuation on the instability and seepage failure of the dump-fill cofferdam, the saturated-unsaturated seepage theory and strength reduction method are embedded into the finite element system such that the fluid-solid coupling stability of the dump-fill cofferdam is analyzed. The results show that the influence of water-level fluctuation on the instability and seepage failure of the dump-fill cofferdam can be revealed by the coupling analysis excellently. The variation of the saturation line of the cofferdam is consistent with the variation of water-level rising, but the change response of the saturation line of the cofferdam has a lag property during the water-level decline process in that the water level changes faster. The maximum displacement of the cofferdam can be approximated as two stages, namely, the stable growth stage and the accelerated growth stage (slip initiation), in which the influence of the water-level fluctuation on the displacement of stable growth stage is more obvious. Based on the fluid-solid coupling analysis, the most dangerous sliding surface of the cofferdam is located at the position of the horse path, with a critical strength reduction coefficient of approximately 1.475. The possibility of seepage failure of the cofferdam will be increased if the water level exceeds the height of the impermeable wall.

1. Introduction

With the development of society, the construction of water conservancy and shipping projects in China is gradually increasing and the scale of construction is expanding. The construction of water conservancy and shipping engineering plays an important role in national economic development and social stability [1–4]. At the same time, the safety of the cofferdam is also crucial, which not only relates to the safety and progress of the whole construction diversion project and the main project but also involves the downstream ecological problems. After nearly 30 years of practice in the construction of large- and medium-sized water conservancy and hydropower projects in China, from the successful interception of the Yangtze River Gezhouba project using the vertical plugging method ([5], [6]) to the construction of the world-renowned Yangtze River Three Gorges project deep-water high earth and stone cofferdam, the design and construction level of diversion and cofferdam engineering has rapidly improved ([7,8]). However, with the continued construction of large and mega hydraulic pivot projects, the scale of cofferdams has increased and the difficulty has grown day by day. The safety and stability of cofferdams are of great concern to researchers and engineers.

As the cofferdams are temporary structures, most of them are made from local materials, generally filled with sand, pebbles, piled stones, and transitional materials, and the more common forms of damage are instability slips and infiltration damage. Therefore, slope stability and seepage stability are two important indicators for evaluating the safety of cofferdams. In terms of research on the stability of cofferdam slopes, Zhao Shangyi et al [9] applied the strength reduction method to slope stability analysis, using the reduction factor when the finite element calculation did not converge as the safety factor, and the analysis results showed that the safety factor of slope stability obtained by this method was quite close to the calculation results of the traditional method. Luo Hongming et al [2] carried out research on the influence of periodic fluctuations of water level on the stability of landslides and proposed a polynomial constrained optimisation model of the soil-water characteristic curve of the polynomial constraint optimisation model applied to actual projects. Yang Jin et al. [10] took the Three Gorges reservoir area loess slope landslide as the research object, carried out the influence of reservoir water rise and fall on the groundwater level of the landslide combined with field monitoring data, and analyzed the influence of the change of the reservoir bank landslide infiltration line on the stability of the landslide under the rise and fall of reservoir water. Xiao Zhiyong et al. [11] took a Three Gorges mound landslide as an example and used Geostudio to analyze the stability of the landslide of a reservoir water-level accumulation body under two factors of multistage descent and different intermittent time periods, and the results showed that the use of intermittent descent was beneficial to the dissipation of pore pressure in the landslide body, while when the reservoir water level decreased rapidly, there was a hysteresis effect of groundwater fall back on the reduction of the hydraulic gradient. Zhang Deng et al. [12] took a tailing pond project as an example and used a time-varying analysis model to study the safety coefficient of the slope, and the results showed that with the change of slope safety coefficient lags behind the change of reservoir water level, the rising speed of water level slowed down the lagging effect, and the falling speed accelerated the lagging effect. And, the decrease in rising rate reduced the lagging effect, and the coupling of rainfall and water level would accelerate the weakening of the tailing reservoir safety coefficient.

This paper relies on the project of Xinjiang River Shuanggang Shipping Hub Project on Poyang Lake in Jiangxi Province. The cofferdam belongs to the dump-fill saturated clay cofferdam, which has the characteristics of high water content of the soil, heterogeneous internal structure, and complex changes in reservoir water level. It is observed that most of the research studies on slope instability of cofferdams are concentrated on mixed types of cofferdams such as soil, rock, and sand and barely concentrated on the research of seepage process and stability of the saturated clay cofferdam. Therefore, there has been an important guiding significance for engineering safety assessment to research the stability and seepage failure of the dump-fill cofferdam caused by water-level fluctuation.

2. Materials and Methods

2.1. Background of the Project. The main construction of this project is located in Poyang Town, Shangrao City, and the width of the riverbed in the dam site area is about 150~450 m. It is a comprehensive hub mainly for navigation. The hub layout is shown in Figure 1, with a total length of 496.5 m along the dam axis. In order to provide dry land construction conditions for the main structure, a diversion canal and a cofferdam should be constructed. The total length of the cofferdam is 2454 m, including 450 m length of the upstream cofferdam, 1459 m length of the longitudinal cofferdam, and 545 m length of the downstream cofferdam, with the service life of the cofferdam which belongs to the perennial cofferdams ranging from 2 to 2.5 years. According to the Design Code for Cofferdams of Water Resources and Hydropower Engineering (SL645-2013), the lock level is Class II and the design level of the cofferdam is Class IV. The weir is protected against seepage by a combination of bagged sand slope protection and geotextile fabric on the headwater side and grass slope protection on the backwater side. The weir body above 19.5 m height is protected against seepage by outsourcing soil filling, and the upstream and downstream weir closed air structure is a high-pressure rotary pile structure; the weir body below 19.5 m height is protected against seepage by a single row of high-pressure rotary pile seepage wall.

2.2. Geological and Hydrological Conditions. According to ground investigation and drilling, the riverbed stratigraphy at the dam site is mainly composed of the Holocene Alluvium of the Fourth Series and the Xinyu Group of the Third Series. The lithology of the original riverbed is divided into chalky clay, thick silty chalky clay medium sand, gravelly sand, rounded gravel, and strong and medium weathered muddy siltstone in order from the top to bottom. The daily water level at the dam site is obtained by interpolation from the water-level stations at Poyang upstream and Longkou downstream of the dam site. Considering the influence of river training before and after 1978 and sand dredging in the lake area and river channel on water-level undercutting in recent years as well as the continuity of the data, the measured water level and the projected flow data of the Shuanggang dam site from Poyang and Longkou stations in the same period after 1991 are used for water level and flow relationship analysis.

2.3. Mechanical Properties of Cofferdam Filling Materials. The saturated clay with silty soil excavated from the diversion channel is the main filling material of the cofferdam, and it has the characteristics of high saturation, high compressibility, and low shear strength because of the double disturbance of excavation and dump-fill so that the cofferdam with a large thickness of 21 m in the upstream and downstream cannot be stable for a long time. In order to construct a stable cofferdam, the outsourcing soil is chosen to fill the upper layer of the cofferdam.

Figure 1: The project overview: layout of the cofferdam diversion channel.

The soil samples are obtained by drilling after the cofferdam was completed, and the physical and mechanical parameters of filling materials are obtained by laboratory tests as shown in Table 1.

3. Seepage Calculation Models

3.1. Saturated-Unsaturated Seepage Theory. The soil of the cofferdam is lying in a complex state of saturation and unsaturation during the water-level fluctuation such that the area which lies below the saturation line can be regarded as saturated and the fluid seepage satisfies Darcy's law and the area which lies above the infiltration line can be regarded as unsaturated and the fluid flow law cannot be given based on Darcy's law. Therefore, the fluid seepage equation should describe both saturated and unsaturated seepage behavior. The continuity equation of the fluid medium during seepage is obtained by taking a volume microelement dV and performing a fluid mass conservation analysis on it [13,14].

$$\int_V \frac{\partial(\rho\theta)}{\partial t} dV + \int_V (\rho \cdot u)_{i,i} dV = \int_V \rho q dV, \tag{1}$$

where θ denotes the volumetric water content, ρ denotes the fluid density, u denotes the fluid percolation velocity, and q denotes the flow rate.

Assuming that the fluid is incompressible during percolation, the previous equation can be evolved as follows:

$$\frac{\partial\theta}{\partial t} + u_{i,i} = q. \tag{2}$$

For a fluid in the saturated zone, the equation of motion is in accordance with Darcy's law:

$$u = -K\nabla h, \tag{3}$$

where K denotes the hydraulic conductivity (coefficient of permeability) and ∇h is the hydraulic gradient.

For fluids in the unsaturated zone, the volumetric water content can be described by the van Genuchten equation [15,16]:

$$\theta = \theta_r + \frac{\theta_s - \theta_r}{\left[1 + (\alpha h)^n\right]^m}, \tag{4}$$

where θ_s and θ_r denote the saturated volumetric water content and residual volumetric water content, respectively, α,m, and n are the basic model parameters, and h is the pressure head which is taken as a positive value.

Substituting equations (3) and (4) into (2), respectively, gives the final form of the equation for fluid seepage continuity in saturated-unsaturated soil.

$$(\theta_s - \theta_r) \cdot \frac{\partial\left[1 + (\alpha h)^n\right]^{-m}}{\partial t} = q + K\nabla h. \tag{5}$$

Equation (5) is a partial differential equation for the pressure head h, which integrates the relationship between the seepage velocity and the matrix suction. However, the partial differential equation is currently difficult to solve analytically and coupled with the dynamic boundary conditions of water-level fluctuation poses a challenge to the solution of the equation. Therefore, it is necessary to solve the equation discretely with the aid of numerical calculations to obtain a numerical solution, so that the seepage state and deformation characteristics of the cofferdam during the water-level fluctuation can be revealed [17].

3.2. Establishment of a Coupled Seepage Model. The model is established based on the closure section of the upstream cofferdam which is regarded as the most dangerous section [18–20]. The height of the cofferdam is 21 m, and the width of the top is 8 m. The length of the upstream face is 43 m, and the ratio of the slope is 1 : 5; the length of the downstream face is 40 m, and the ratio of the slope is 1 : 4~1 : 5. The soil types from the top to the bottom are gravelly silty clay, fill material, silty clay, medium sand, rounded gravel, and strongly weathered muddy siltstone (as shown in Figure 2). To prevent infiltration damage to the cofferdam and ensure its stability, two rows of interlocking high-pressure jet grouting piles were installed 1.5 m below the top of the cofferdam, with a width of 0.8 m and a depth of 2 m inside the strongly weathered rock, providing good

Table 1: Basic physical and mechanical parameters of cofferdam, rock, and soil.

Cofferdam materials	Cohesion (kPa)	Angle of internal friction (°)	Coefficient of permeability (cm/s)	Natural gravity (kN/m^3)	Saturated bulk weight (kN/m^3)	Modulus of elasticity (kPa)	Poisson's ratio
Outsourced soil	21.23	10.03	6.63×10^{-5}	18.40	19.30	10240	0.3
Fill material	13.47	7.40	9.27×10^{-8}	19.70	19.70	8820	0.3
Powdery clay	20.00	13.00	7.0×10^{-5}	18.80	20.00	8640	0.3
Medium sand	0.00	28.00	1.0×10^{-3}	18.00	19.00	12000	0.3
Round gravel	0.00	35.00	1.0×10^{-2}	18.60	19.60	36000	0.3
Impregnating wall	/	/	5.0×10^{-9}	22.00	23.00	300000	0.2
Strongly weathered rock	100.00	35.00	1.0×10^{-4}	20.00	21.00	300000	0.3

impermeability. The basic physical and mechanical parameters of the materials are detailed in Table 1.

The COMSOL Multiphysics software is used to analyze the seepage and stability of the cofferdam, and the model is established as shown in Figure 3. The analysis of saturated-unsaturated seepage can be accomplished based on the PDE module which embedded Equation (5). The Mohr–Coulomb ontology model is used for the geotechnical materials, the effects of fluid osmotic pressure and the self-weight of the geotechnical materials are considered, and the coupling calculation is accomplished as follows:

$$\begin{cases} F = \lambda\sqrt{J_2} + \varpi I_1 - \chi \\ \varpi = \sin\varphi/3, \chi = c/\cos\varphi \end{cases}, \tag{6}$$

where F denotes the Mohr–Coulomb yield function, c and φ denote the cohesion and internal friction angle of the geotechnical materials, and J_2 and I_1 denote the second invariant of partial stress and the first invariant of stress, respectively.

In order to carry out the subsequent stability analysis of the cofferdam, a shear strength reduction factor (Equation (7)) is introduced to discount the mechanical parameters of the geotechnical materials until the destruction occurs [21].

$$\begin{cases} C = \dfrac{c}{\xi} \\ \Phi = a\tan\left(\dfrac{\tan\varphi_u}{\xi}\right)_{p<0} + a\tan\left(\dfrac{\tan\varphi_s}{\xi}\right)_{p\geq 0} \end{cases}. \tag{7}$$

Here, ξ denotes the strength discount factor, φ_u and φ_s are the internal friction angles of unsaturated and saturated geotechnical bodies, p denotes the pore pressure, and C and Φ are the cohesion and internal friction angles after considering the strength discount.

3.3. Boundary Conditions of Displacement and Pressure. The bottom of the model is constrained by fixed displacement with zero displacement boundary; the model is surrounded by roller displacement constraint with zero normal displacement.

$$for\begin{cases} z = z_b: & U_x = U_y = 0 \\ z \neq z_b: & U_x = 0. \end{cases} \tag{8}$$

The boundary condition of water pressure at the upstream face is related to the water level which changed with time. For this reason, we research the water-level fluctuation data of Poyang Lake in the last 40 years and find that the water-level fluctuation rates of 1998 are the most drastic. The highest flood level is 20.76 m, which is only 0.24 m away from the top of the cofferdam; the lowest water level is 11.60 m, the difference between flood and dry water level reaches 9.16 m, and the pressure difference is 90.16 kPa, which has a huge impact on the cofferdam of the throw-fill type powder clay with silt soil. It is necessary to carry out a destabilization and infiltration damage study for the upstream cofferdam where the water-level difference is large.

Figure 4(a) shows the water-level variation of the lake in 1998. The flooding season lasts from June to August each year, while winter and spring are the low-water-level seasons. Considering the large discreteness of the actual data that the calculation speed and astringency of the model would be impacted significantly, the highest water level of each month is taken as the reference value (the most dangerous case) and interpolated for analysis, resulting in the water-level change curve shown in Figure 4(b). The similarity index of them is 90%, and the timing of the flood and dry water levels coincide exactly, which has an approximately negligible effect on the model calculations.

3.4. Calculation Parameters and Simulation Conditions. The physical and mechanical parameters and infiltration parameters of the cofferdam are detailed in Table 1, and the water-level depth and fluctuation rates are given in Figure 4(b). In terms of numerical analysis, three groups of scenarios are set up, which are the steady-state simulations at the lowest and highest water levels and the transient simulations at the dynamic fluctuation of the water level over a year; the detailed simulation scenarios are shown in Table 2.

In particular, for the transient coupling calculation under the dynamic rise and fall of the water level, the initial seepage field of the weir body needs to be given. Here, the water level of the first day in 1998 (12.92 m) is taken as the initial seepage condition, the initial seepage field and stress field conditions are obtained through the steady-state

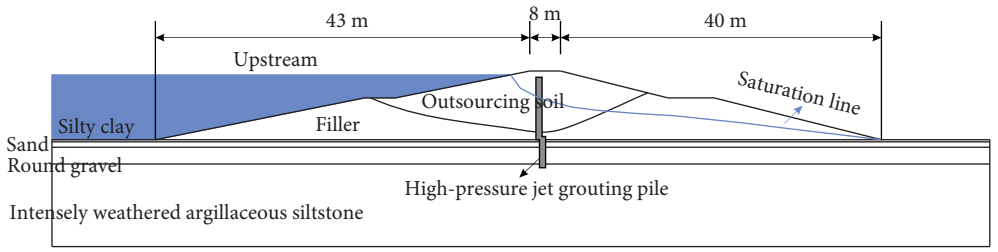

Figure 2: Lateral section of the upstream closure section of the cofferdam.

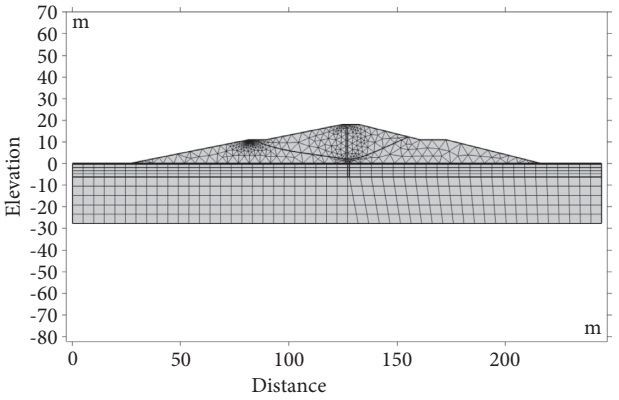

Figure 3: Fluid-solid coupling numerical analysis model.

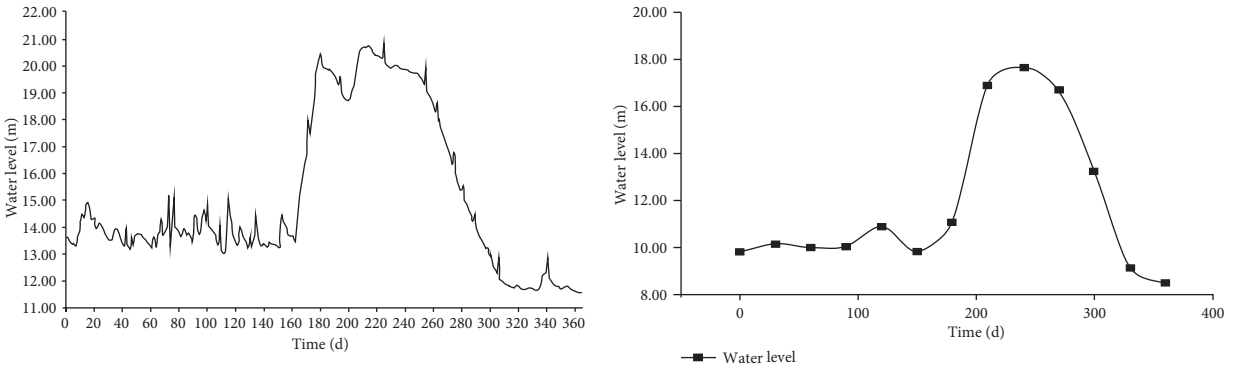

Figure 4: Change trend of water level of the cofferdam: (a) actual water-level change; (b) simplified water lever based on interpolation.

Table 2: Simulation conditions.

Simulation program	Water-level position (m)	Water level in foundation pit (m)	Computational simulation
Minimum water level	11.60	Pit bottom-1 m	Steady-state coupling
Maximum water level	20.76	Pit bottom-1 m	Steady-state coupling
Dynamic water level	11.60~20.76	Pit bottom-1 m	Transient coupling

coupling calculation, and then, the purpose of the transient coupling calculation is achieved [22].

4. Analysis of Results and Discussion

4.1. Influence of Water-Level Fluctuation on the Saturation Line of the Cofferdam. The variation of pore water pressure and saturation line in the cofferdam can be obtained by steady-state coupling and a transient coupling according to different simulation conditions. Figures 5 and 6 show the variation of pore water pressure and saturation line in the cofferdam at the lowest and highest water levels, respectively. The comparative analysis shows that the water level has a significant influence on the seepage rate, pore water

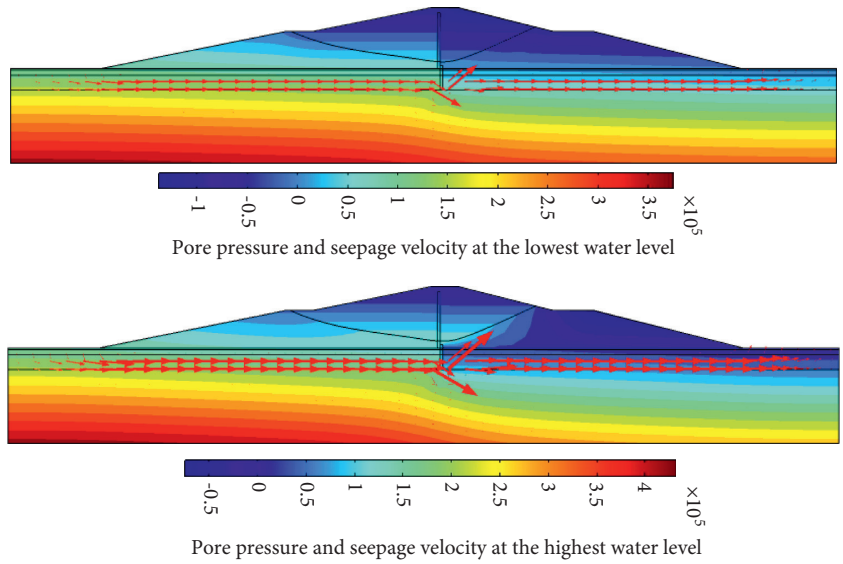

Figure 5: Contour map of pore pressure and seepage velocity in the cofferdam.

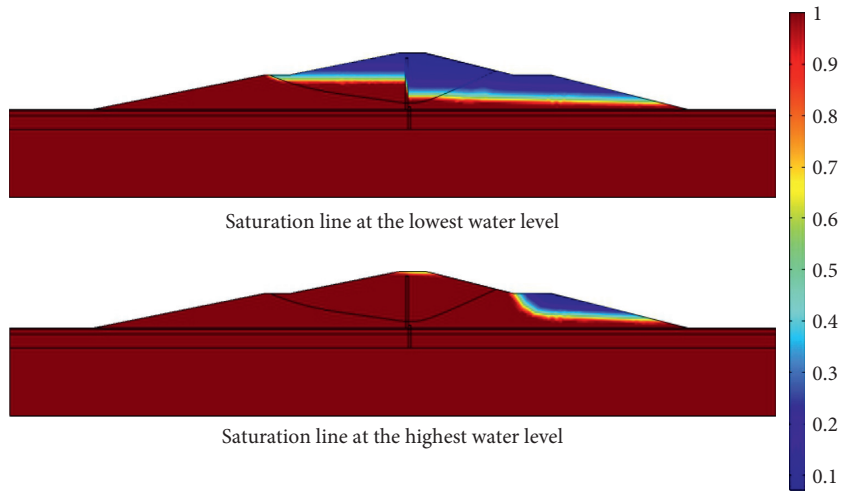

Figure 6: Contour map of the seepage line in the cofferdam.

pressure, and infiltration line in the cofferdam. The higher the water level is, the more saturated the areas (red areas) are, the faster the seepage rate (flow rate arrows) is, and the more drastic the pore pressure change will be. Due to the setting of the high-pressure cyclone wall, there are obvious sudden changes in pore water pressure and regional saturation between the different sides of the impermeable wall, the seepage area is mainly concentrated in the medium sand and round gravel layer, and the phenomenon of bypass flow exists at the bottom of the wall, which has a positive seepage prevention effect. With the gradual increase in water level, the water pressure gradient in the cofferdam is increased, and when the water level exceeds the impermeable wall, the effect of seepage prevention and flow blocking of the impermeable wall is gradually weakened and the stability of the cofferdam will be decreased.

The variation of the saturation line of the cofferdam under the dynamic water-level fluctuation condition is shown in Figure 7, and the variation regulation of the saturation line is similar to the water-level fluctuation regulation which is shown in Figure 4(b), illustrating that the migration of moist sharp in the cofferdam is controlled by the water-level fluctuation. During the flood period from June to August, the water level rises rapidly and fluid flow occurs along the outsourcing soil of the cofferdam, resulting in an increase in the saturated zone on the right side, with the unsaturated zone only existing near the bottom of the slope inside the cofferdam. In addition, due to the saturated-unsaturated soil seepage theory model used, the saturation line that migrates in the cofferdam has significant lagging characteristics during the water-level decline process; for example, the water level in September is lower than the water level in July, but its saturation zone is larger than that in July, which is not consistent with the water-level rising regulation; the water level in November is the same as the water level in May, but the saturation line in the cofferdam does not

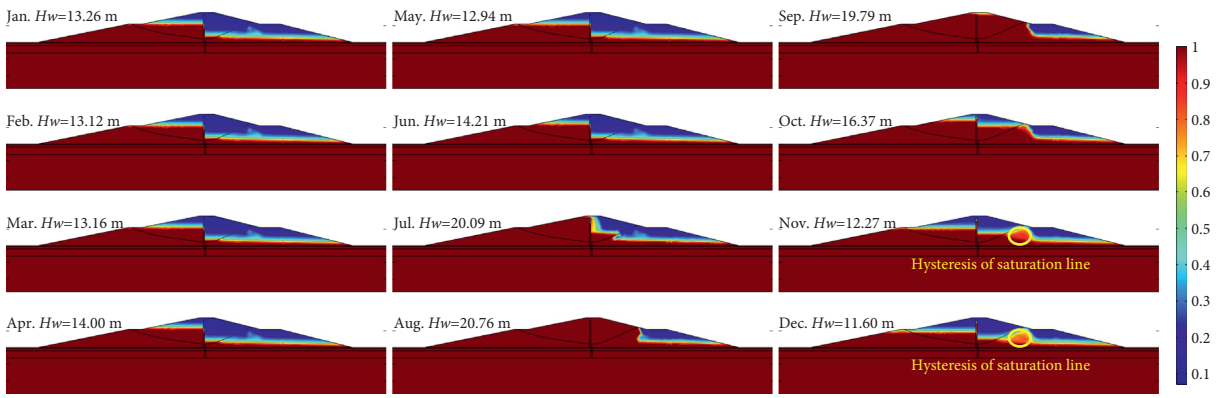

Figure 7: Change of the seepage line in the cofferdam under water-level fluctuation.

exactly overlap either. The results show that there are different effects on the saturation line caused by water-level rising and decline and the effect caused by the water-level decline process is more significant.

4.2. Influence of Water-Level Fluctuation on the Displacement of Cofferdam. The analysis points of displacement in the cofferdam model are selected as shown in Figure 8, where Section 1-1 indicates the downstream face, Section 2-2 indicates the intersection between the outsourcing soil and the fill material, Section 3-3 indicates the vertical section at the top of the cofferdam, and Section 4-4 indicates the vertical section at the horse path. The blue points shown in Figure 8 are the key points for slide damage that locate on the surface or at the intersection of different geotechnical materials.

The deformation results of the four sections of the cofferdam are shown in Figure 9. The results indicate that the water-level fluctuation has a light influence on the deformation of the top of the cofferdam, which remains at 17.16 mm. But it has an obvious influence on the deformation of the intersection of geotechnical materials. For example, during the flood period, the displacements of the intersection of outsourcing soil and filler (points B, J, and E), the intersection of medium sand and round gravel (points C and H), and the intersection of round gravel and strongly weathered muddy siltstone (point *D* and I) show significant increase such that the maximum displacement increment is about 11.62 mm which is located in point J. In general, the deformation values of the cofferdam meet the safety requirements and the probability of seepage damage is slight. But special attention needs to be paid to the deformation between the intersection of the outsourced soil and the filler, which is the potential slip surface of the cofferdam.

4.3. Influence of Water-Level Fluctuation on the Stability of the Cofferdam. The highest and lowest water-level conditions and the shear strength reduction method are used to analyze the stability of the cofferdam. The evaluation of whether the cofferdam has slide damage is relied on the shear strength reduction factor, and there is no convergence of elastic-plastic analysis of geotechnical materials as the referee condition. The analysis results show that the maximum displacement of the cofferdam increases slowly as the strength reduction factor gradually increases, and when the reduction factor reaches a certain threshold value, the maximum displacement rises sharply, which means that slip damage begins. The reduction factor that causes the sudden increase in the maximum displacement is named the critical strength reduction factor (CSRF).

The variation curves of the maximum displacement of the cofferdam with the strength reduction factor under the highest and lowest water-level conditions are shown in Figure 10. The curves can be divided into two stages. During the first stage, the maximum displacement is increasing stably and the displacement in the highest water-level condition is a little larger than that in the lowest water-level condition. The maximum displacement in the second stage is increasing rapidly, and the curves in two different conditions are coincident such that the slide is forming. The result means that the water level has almost no effect on the critical strength reduction factor of the cofferdam, which is about 1.475.

Figure 11 shows the effective plastic strain of the cofferdam before the destruction at the highest and lowest water levels, respectively, which is another representation of the cofferdam damage mechanism. The effective plastic strain variation of the two different conditions are consistent, and this result is consistent with the results of the critical strength discount factor analysis. Figure 12 shows the slide surface of the cofferdam under the highest and lowest water-level conditions, respectively, with the most dangerous slide surfaces being located at the horse path and the arrows indicating the direction of displacement of the soil particles. The most dangerous slide surface for both conditions is also in general agreement and also coincides with the results of the effective plastic strain and critical strength reduction factor analysis.

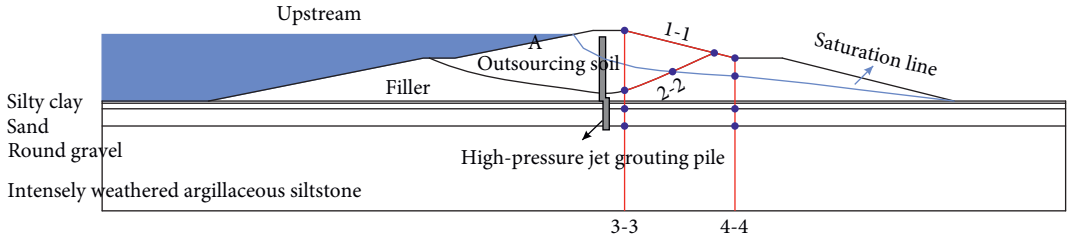

Figure 8: Schematic diagram of selection of cofferdam deformation analysis points underwater-level fluctuation.

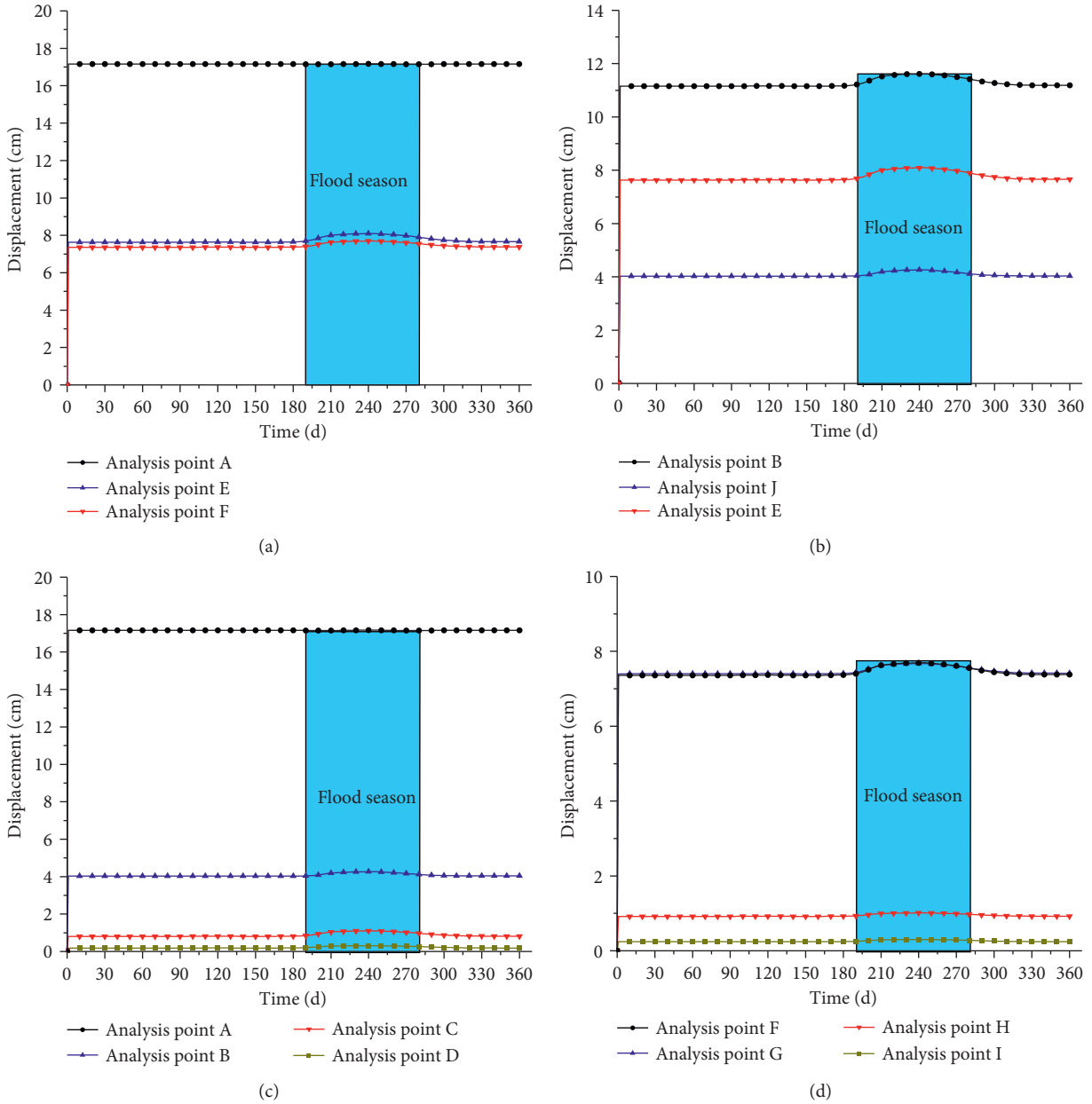

Figure 9: Schematic diagram of selection of cofferdam deformation analysis points underwater-level fluctuation: (a) deformation of the backwater slope of the cofferdam; (b) deformation of the interface between outsourcing oil and the filler; (c) vertical section deformation at the top of the cofferdam; (d) vertical section deformation at the horse track.

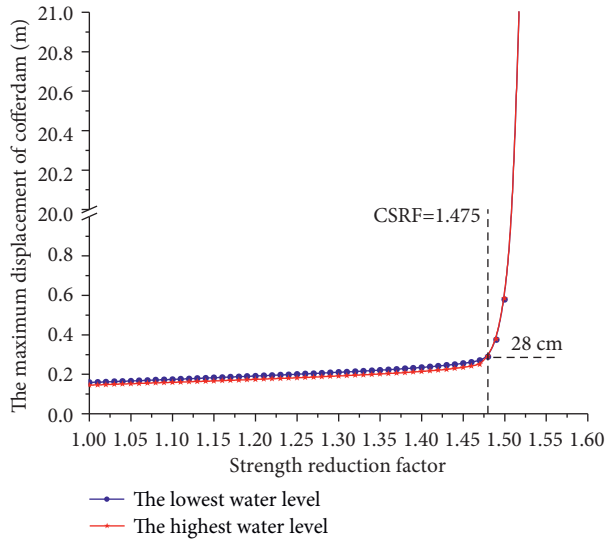

Figure 10: The variation law of the maximum displacement of the cofferdam with the strength reduction factor.

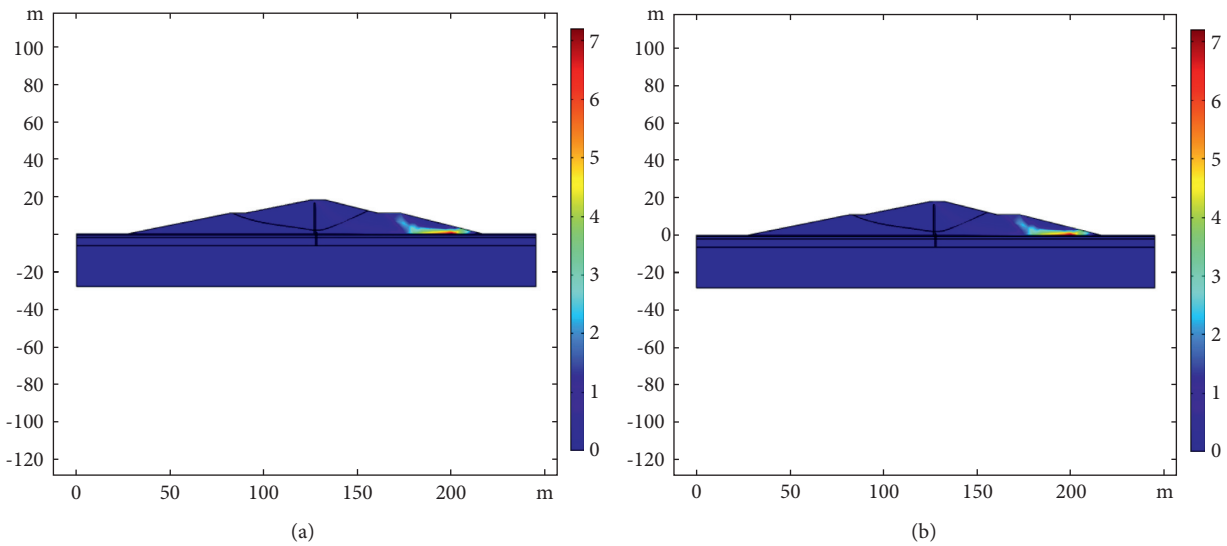

Figure 11: The effective plastic strain before the cofferdam failure under (a) flood level and (b) low water level.

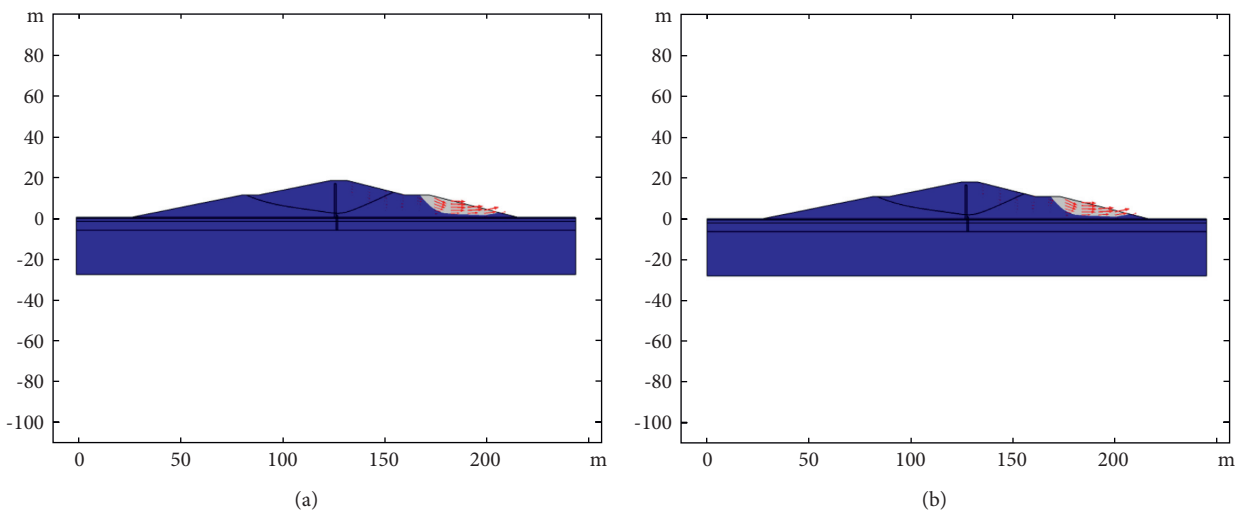

Figure 12: The most dangerous slip surface of the cofferdam under (a) flood level and (b) low water level.

5. Conclusion

(1) The influence of water-level fluctuation on the deformation and stability of the cofferdam can be analyzed excellently by finite element simulation which embedded the saturated-unsaturated seepage theory.

(2) With the rise of water level, the saturation zone in the cofferdam increases and the value of pore water pressure changes sharply. The prevention effect of the impermeable wall will be reduced while the water level exceeds the top of the impermeable wall, and the saturation zone of the downstream face will be enlarged, causing the decrease in stability of the cofferdam.

(3) The variation regulation of the saturation line is similar to the water-level fluctuation regulation, and the migration of moist sharp in the cofferdam is controlled by the water-level fluctuation. Because of the use of saturation-unsaturation seepage theory, the saturation line in the cofferdam lags to the water-level fluctuation and the lag time is more obvious during the water-level decline process.

(4) The maximum displacement of the cofferdam can be divided into two stages: stable increasing stage and sharp increasing stage. The maximum displacement in the second stage is increasing rapidly, and the curves in two different conditions are coincident such that the slide is forming. The result shows that the water level has almost no effect on the critical strength reduction factor of the cofferdam, which is about 1.475.

Data Availability

The data reported in this article are available from the corresponding author upon request.

Conflicts of Interest

The authors declare that they have no conflicts of interest.

Acknowledgments

This work was supported by Key Engineering Science and Technology Projects of Jiangxi Provincial Department of Transportation (2019C0010 and 2019C0011); National Natural Science Foundation of China (51868021 and 52168047); Jiangxi Provincial Natural Science Foundation (20202BABL20405); High Speed Railway Joint Fund of NSFC (U1934208); and Natural Science Foundation of Jiangxi Province (20212BAB214009).

References

[1] X. Bai, *Research on the Evaluation of China's Soft Power of Shipping*, Dalian Maritime University, Dalian, 2013.

[2] H. Luo, H. Tang, and G. Zhang, "Influence of reservoir water level rise and fall on the stability of reservoir bank landslides," *Earth Science*, vol. 33, no. 5, pp. 687–692, 2008.

[3] B Wang, D Huang, and H Jian, "Social stability risk assessment and empirical study of water conservancy project construction," *China Population Resources and Environment*, vol. 25, no. 4, pp. 149–154, 2015.

[4] H. Xie, W. Xu, and C. Liu, "Strategic concept and key technology outlook for underground hydraulic engineering," *Journal of Rock Mechanics and Engineering*, vol. 37, no. 4, pp. 781–791, 2018.

[5] H. Guo, J. Ning, and W. Jiang, "Experimental research and engineering practice on the protection (mat) bottom of the interceptor dragon mouth of large water conservancy projects," *Journal of China Three Gorges University*, vol. 29, no. 6, pp. 481–485, 2007.

[6] D. M. Liu, D. Y. Wang, and X. M. Wang, "Experimental study and basic conclusions of some hydraulics problems of the Grand River cut-off of Gezhouba project," *Chinese Science (Series A) Mathematics Physics Astronomy Technology Science*, vol. 10, pp. 951–962, 1982.

[7] H. Dai and L. Wang, "Study of seepage in the Three Gorges deep-water high earth and rock weir project," *Advances in Water Science*, vol. 16, no. 6, pp. 849–852, 2005.

[8] Si Zhaole, "Science and technology of deep water high earth and rock cofferdam of Three Gorges Project Phase II and its practical test," *Journal of Yangtze River Scientific Research Institute*, vol. 21, no. 6, pp. 1–6, 2004.

[9] S. Zhao, Y. Zheng, and W. Shi, "Coefficient of safety for slope stability using finite element strength reduction," *Chinese Journal of Geotechnical Engineering*, vol. 3, pp. 343–346, 2002.

[10] Y. A. N. G Jin, W. Jian, and H. Yang, "Study on the dynamic change of infiltration line of loess slope in Three Gorges reservoir area," *Rock and Soil Mechanics*, vol. 33, no. 3, pp. 853–858, 2012.

[11] Z. Xiao, H. Deng, and J. Li, "Influence of intermittent decline in reservoir water level on the stability of mounded landslides," *Journal of the Yangtze River Academy of Sciences Scientific Research Institute*, vol. 33, no. 8, pp. 114–119, 2016.

[12] D. Zhang, W. B. Jian, and Q. Ye, "Time-varying analysis model of tailings pond slope and its application," *Rock and Soil Mechanics*, vol. 35, no. 3, pp. 835–840, 2014.

[13] X. Kong, *Higher Seepage Mechanics*, Press of University of Science and Technology of China, Hefei, 2010.

[14] Q. W. Zhan and R. D. Liu, "Research on slope instability during rainfall," *Yangtze River*, vol. 42, no. 11, pp. 103–106, 2011.

[15] H. Li, J. Q. Wu, and R. Hou, "Experimental study on the application of one-step flow method for rapid determination of soil-water characteristic curve," *Yangtze River*, vol. 51, no. 2, pp. 160–165, 2020.

[16] Z. Tian, D. Kool, T. Ren, R. Horton, and J. L. Heitman, "Approaches for estimating unsaturated soil hydraulic conductivities at various bulk densities with the extended Mualem-van Genuchten model," *Journal of Hydrology*, vol. 572, pp. 719–731, 2019.

[17] Y.G. Zhang, J. Tang, Y. M. Cheng et al., "Prediction of Landslide Displacement with Dynamic Features Using Intelligent Approaches," *International Journal of Mining Science and Technolog*, vol. 2, no. 1, pp. 1–11, 2022.

[18] G. Han, Y. Zhou, R. Liu, Q. Tang, X. Wang, and L. Song, "Infuence of surface roughness on shear behaviors of rock joints under constant normal load and stifness boundary conditions," *Natural Hazards*, vol. 2, no. 1, pp. 1–18, 2022.

[19] L. XL, C. SJ, Z. QM, and G. X Feng F., "Research on theory, simulation and measurement of stress behavior under

regenerated roof condition," *Geomechanics and Engineering*, vol. 26, no. 1, pp. 49–61, 2021.

[20] H. Wu, G. Zhao, and S. Ma, "Failure behavior of horseshoe-shaped tunnel in hard rock under high stress: Phenomenon and mechanisms," *Transactions of Nonferrous Metals Society of China*, vol. 32, no. 2, pp. 639–656, 2022.

[21] S. Li, Y. G. Zhang, M. Cao, and Z. N. Wang, "Study on excavation sequence of pilot tunnels for a rectangular tunnel using numerical simulation and field monitoring method," *Rock Mechanics and Rock Engineering*, vol. 12, pp. 1–16, 2022.

[22] B. Yang, M. He, Z. Zhang, J. Zhu, and Y. Chen, "A New Criterion of Strain Rockburst in Consideration of the Plastic Zone of Tunnel Surrounding Rock," *Rock Mechanics and Rock Engineering*, vol. 14, pp. 1–15, 2022.